

## Crustal thinning of the northern continental margin of the South China Sea

Ching-Hui Tsai<sup>1,2</sup>, Shu-Kun Hsu<sup>1</sup>, Yi-Ching Yeh<sup>1</sup>, Chao-Shing Lee<sup>2</sup> and Kanyuan Xia<sup>3</sup>

<sup>1</sup>*Institute of Geophysics, National Central University, Taiwan*

<sup>2</sup>*Institute of Applied Geosciences, National Taiwan Ocean University, Taiwan*

<sup>3</sup>*South China Sea Institute of Oceanology, Chinese Academy of Sciences, China*

(E-mail: [chtsai@oc.gep.ncu.edu.tw](mailto:chtsai@oc.gep.ncu.edu.tw))

Received 28 January 2004; accepted 1 September 2004

**Key words:** continental margin, crustal structure, crustal thinning, gravity modeling, South China sea

### Abstract

Magnetic data suggest that the distribution of the oceanic crust in the northern South China Sea (SCS) may extend to about 21 °N and 118.5 °E. To examine the crustal features of the corresponding continent–ocean transition zone, we have studied the crustal structures of the northern continental margin of the SCS. We have also performed gravity modeling by using a simple four-layer crustal model to understand the geometry of the Moho surface and the crustal thicknesses beneath this transition zone. In general, we can distinguish the crustal structures of the study area into the continental crust, the thinned continental crust, and the oceanic crust. However, some volcanic intrusions or extrusions exist. Our results indicate the existence of oceanic crust in the northernmost SCS as observed by magnetic data. Accordingly, we have moved the continent–ocean boundary (COB) in the northeastern SCS from about 19 °N and 119.5 °E to 21 °N and 118.5 °E. Morphologically, the new COB is located along the base of the continental slope. The southeastward thinning of the continental crust in the study area is prominent. The average value of crustal thinning factor of the thinned continental crust zone is about 1.3–1.5. In the study region, the Moho depths generally vary from ca. 28 km to ca. 12 km and the crustal thicknesses vary from ca. 24 km to ca. 6 km; a regional maximum exists around the Dongsha Island. Our gravity modeling has shown that the oceanic crust in the northern SCS is slightly thicker than normal oceanic crust. This situation could be ascribed to the post-spreading volcanism or underplating in this region.

### Introduction

The South China Sea (SCS) is the largest marginal sea off East Asia. It is surrounded by south China, Taiwan, the Luzon arc, Palawan and the Indo-China peninsula (Figure 1). In general, the SCS can be divided into the northern continental margin, the central oceanic basin and the southern continental margin. Yan et al. (2001) suggested the northern and southern margins of the SCS make an asymmetric conjugated pair and the northern part can be classified as non-volcanic margin. In contrast, Clift et al. (2001) showed that there is excess volcanism and that it is not non-volcanic beneath the northern continental margin of the SCS. Nissen et al. (1995a) and Kido et al. (2001) also indicated the existence of underplating. The continental rifting of the East Asian margin has resulted in a series of extensional basins in East Asian margin (Sibuet and

Hsu, 1997). The Pearl River Mouth Basin (PRMB) is largely distributed in the continental shelf of the northern SCS (Figure 1). Dongsha Island is located in the middle of the northern continental margin (Figure 1). East of Dongsha Island, the physiography is marked by the presence of the Formosa Canyon (FC) and the Manila Trench (Figure 1). Formosa Canyon has developed along the northwest part of the LRTPB (Luzon-Ryukyu Transform Plate Boundary) (Hsu et al., 2005). West of Dongsha Island, the Xisha Trough is a distinct bathymetric depression and was interpreted as a locus of crustal rifting (Taylor and Hayes, 1983) (Figure 1). Nissen et al. (1995a) showed that the Xisha Trough is a thick sedimentary basin with thin igneous crust.

The oceanic crust in the central SCS basin was formed by seafloor spreading between 32 and 15 Ma (Briaies et al., 1993). Except the northeast

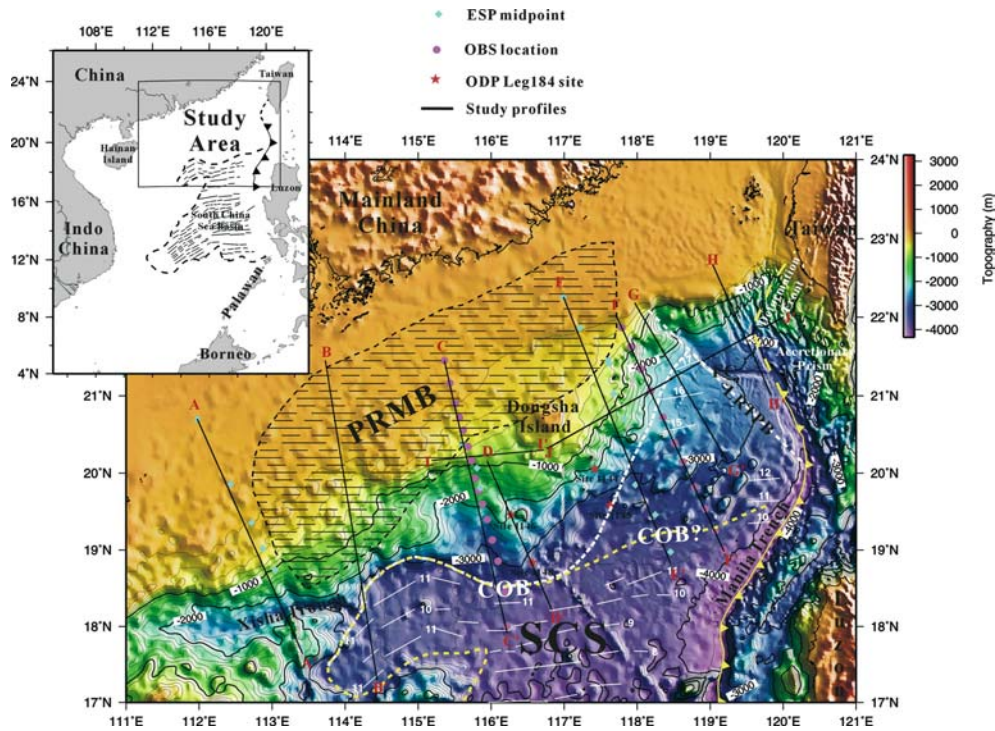


Figure 1. Schematic map of the major tectonic configuration of northern South China Sea (SCS). The yellow dashed line indicates the continent–ocean boundary (COB) suggested by Briais et al. (1993). The white dashed line is our preferred COB. The black lines are locations of the crustal or seismic profiles used in this study. The data sources are described in Table 1. The white thin lines indicate the magnetic anomalies. PRMB: Pearl River Mouth Basin. FC: Formosa Canyon. L RTPB: Luzon-Ryukyu Transform Plate Boundary (Sibuet et al., 2002).

and southeast corners of the SCS, the continent–ocean boundary (COB) of the SCS defined by Briais et al. (1993) almost coincides with the 3000 m-isobath, near the base of the continental slope (Figure 1). However, due to lack of good correlated magnetic data and deep seismic profiles, most previous studies did not suggest the existence of oceanic crust in the area between Dongsha Island and Taiwan. Based on recent magnetic study, the distribution of SCS oceanic crust has been identified to the north of the COB suggested by Briais et al. (1993) and the age of the oceanic crust could be as old as 37 Ma (Hsu et al., 2004). However, the crustal structure across the continental margin of the northernmost SCS was rarely studied.

The main objective of this study is to give a comprehensive understanding of the crustal features of the northern continental margin of the SCS. For that, we have conducted new seismic reflection profiles between Dongsha Island and Taiwan and combined these with several previous

profiles. Most of the profiles used are across the continental shelf, the continental slope and the deep ocean basin. We also performed gravity modeling to understand the Moho depth distribution and the variation of crustal thicknesses across the northern margin of the SCS.

### Seismic data

To have an overview of the crustal structures in the northern margin of the SCS, we use six existing seismic profiles or crustal models and two new seismic reflection profiles (Figures 2–6) (Table 1). Profiles AA', BB', CC', and EE' (Table 1) are crustal models from Nissen et al. (1995a), Yan et al. (2001), Ludwig et al. (1979) and Taylor and Hayes (1983). Profiles DD' and HH' (Table 1) are MCS (Multi-Channel Seismic) profiles from Lüdmann et al. (2001) and Sibuet et al. (2002), respectively. All these profiles or crustal models are across the continental shelf, the continental slope, and some deep ocean basin

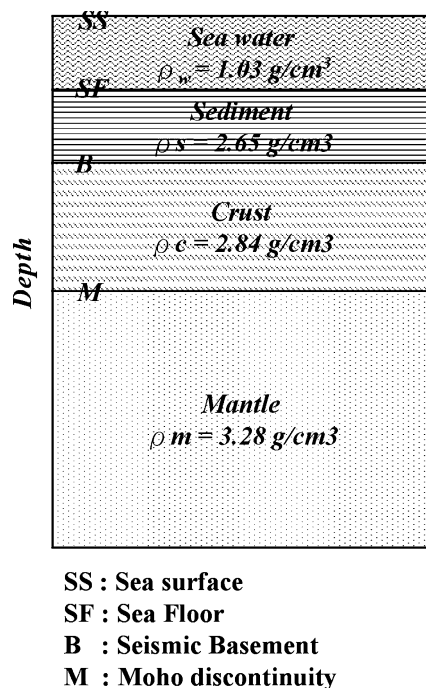


Figure 2. A simple four-layer crust model used for gravity modeling in this study.

(Figure 1). The two new profiles contain a wide-angle seismic refraction and MCS reflection survey (MLTW-OBS cruise) in August 2001 and a MCS seismic survey (MCS689 cruise) in July 2003. Both two surveys were conducted in the northernmost SCS (Figure 1) (Table 1). We used ProMax seismic software and SIOSEIS (Henkart, 1992) to process these two new seismic profiles. Using all the available profiles, we can delineate the continental crust (CC) zone, the thinned continental crust (TCC) zone, the oceanic crust (OC) zone, and the COB location in the northern SCS.

## Gravity and magnetic data

To simulate the variation of crustal thickness across the northern continental margin of the SCS, we adopt a simple four-layer crustal model (Figure 2). Taking into account the results of Nissen et al. (1995b), we assume the densities of sea water, sediment, crust and upper mantle to be  $\rho_w = 1.03 \text{ g/cm}^3$ ,  $\rho_s = 2.65 \text{ g/cm}^3$ ,  $\rho_c = 2.84 \text{ g/cm}^3$  and  $\rho_m = 3.28 \text{ g/cm}^3$ , respectively. We use the satellite-derived gravity anomalies of Sandwell and Smith (1997) (Figure 9c and 9d). We calculate the Bouguer anomaly along each profile by subtracting the gravity effect of seawater/sediment and the sediment/basement interfaces from the free-air gravity anomaly. The Bouguer anomaly corresponds to the gravity effect from the variation of the Moho discontinuity surface. Hence, the Moho depth variation of each profile is found by fitting the synthetic Bouguer anomaly and the Bouguer anomaly in the sense of least square error. The results are shown in Figure 8. The magnetic anomaly along each profile is plotted. We have used two magnetic data sources: one from the Coordinating Committee for Geoscience Programmes in East and Southeast Asia (CCOP) and the other from Hsu et al. (1998) (Figure 8a–8f from CCOP and Figure 8g–8h from Hsu et al., 1998).

## Crustal structures across the continental margin

In the following sections, we interpret the crustal structures along each profile from the west of the study area to the east (Figure 1).

Table 1. The seismic profiles used for gravity modeling

Profile name	Profile description
AA'	Modified from western transect of the ESPs (Nissen et al., 1995 a, b)
BB'	Modified from geological transect (Ludwig et al., 1979; Taylor and Hayes, 1983)
CC'	Modified from crustal model by OBS (Yan et al., 2001)
DD'	Modified from SO95-5 MCS profile of the SO-95 cruise (Lüdmann et al., 2001)
EE'	Modified from eastern transect of ESPs (Nissen et al., 1995 a, b)
FF'	The mlw post-stack MCS profile of the co-operated MLTW-OBS cruise between Taiwan and China in 2001
GG'	The mcs689-5 post-migrated MCS profile of the MCS689 cruise in 2003
HH'	Modified from EW9509-45 MCS profile of the EW9509 cruise (Sibuet et al., 2002)

ESPs: Expanding Spread Profiles; MCS: Multi-Channel Seismic; OBS: Ocean Bottom Seismometer.

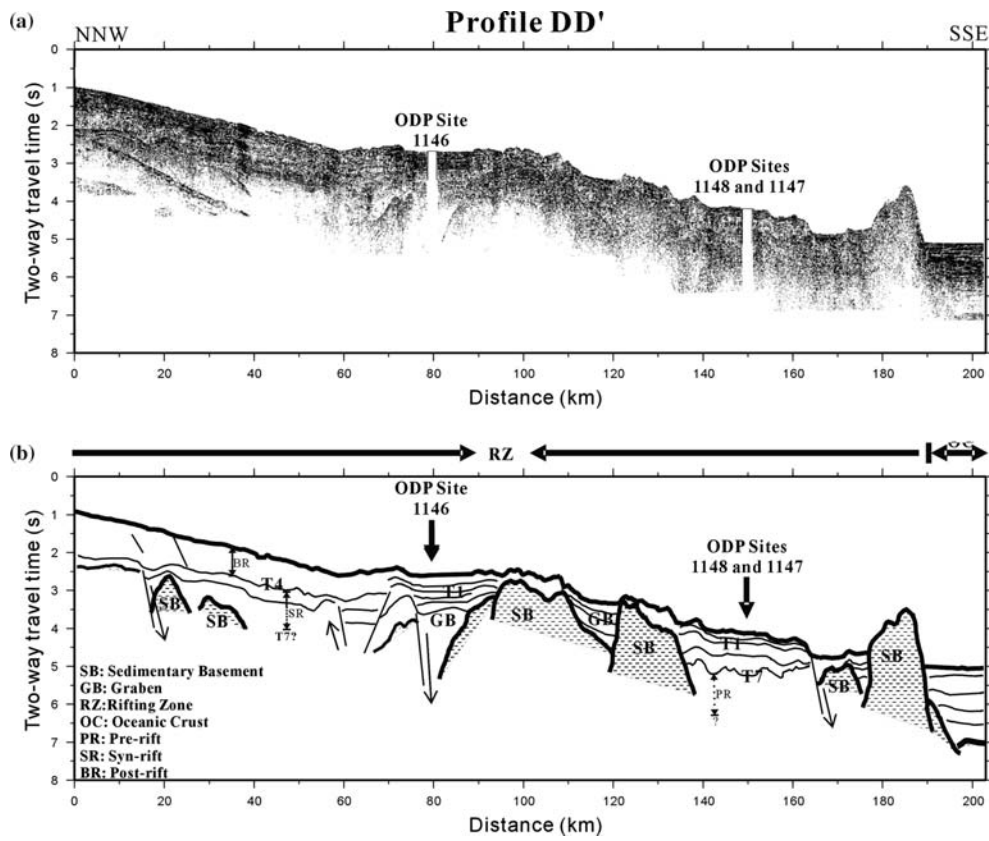


Figure 3. (a) Seismic Profile DD' and (b) the interpretation of Profile DD'. This profile is modified from Lüdmann et al. (2001). Several grabens filled with thick sediments are observed.

#### Profile AA' (Figure 8a)

The profile in Figure 8a was interpreted by Nissen et al. (1995a, b). Several failed spreading centers have been found (boxes A1, B1, C1 in Figure 8a) (Taylor and Hays, 1983). Faults across the entire crust have been suggested near the failed spreading centers (Nissen et al., 1995b). For comparison, we use the Moho depth defined by Nissen et al. (1995a) to calculate the synthetic Bouguer gravity anomaly (the heavy dashed line in Figure 8a). Except the short-wavelength anomalies, the result shows a good fitting between calculated and synthetic Bouguer anomaly curves. At a distance between 270 and 370 km along the profile is located the Xisha Trough. Beneath the Xisha Trough, a failed spreading center, the mantle has been uplifted and the crust has been thinned from ca. 28 km to 8 km thick (box C1). The corresponding Bouguer anomaly above the Xisha Trough is high (box C2 area). The anomaly

ously low free-air anomaly (box C2 in Figure 8a) however shows the subsidence or thinning effect of the upper crust. The magnetic anomaly shows strong amplitude above the Xisha Trough (box C3 in Figure 8a); however, no oceanic crust is suggested along this profile.

#### Profile BB' (Figure 8b)

As shown in profile Figure 8b, the Bouguer anomaly becomes larger oceanwards. Accordingly, the Moho depth must be shallower oceanwards. The gravity modeling indicates that the thin crust of about 6 km corresponding to oceanic crust is located after distance 350 km (boxes C1 in Figure 8b). Above the oceanic crust, the reversal pattern of the magnetic anomaly is prominent (box C3 in Figure 8b). Between distances 290 and 350 km, the continental crust has been thinned dramatically. This portion is considered as thinned continental crust (TCC) zone, which is located

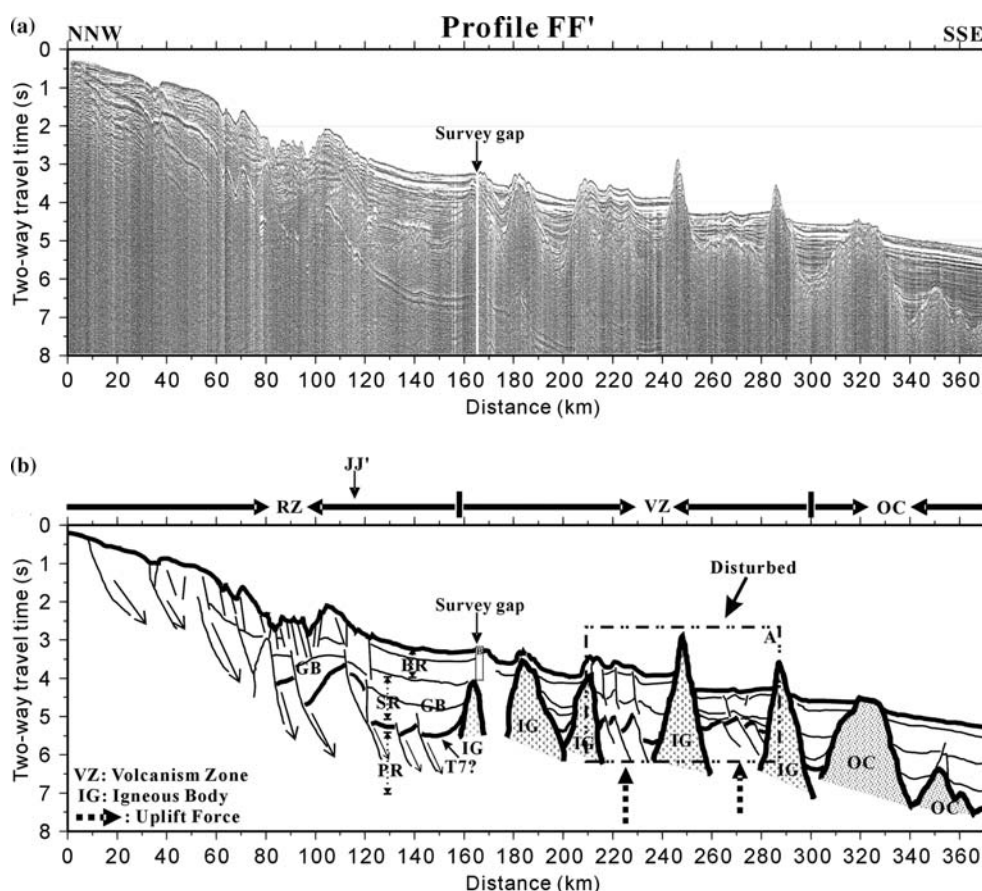


Figure 4. (a) Seismic profile FF' and (b) the interpretation of profile FF'. There are many intruded and extruded igneous bodies (IG) in this profile. Tilted, rotated normal faults are found near the basement. OC: oceanic crust. GB: graben. PR: pre-rift. SR: syn-rift. BR: post-rift.

between the non-deformed or slightly deformed continental crust and the oceanic crust (Figure 8b). Slight deformation due to the continental rifting can also be observed in boxes A and B of Figure 8b. In this profile, the continental crust (CC) zone is defined as the area from distance 0 to 290 km (Figure 8b).

#### Profile CC' (Figure 8c)

The depth to the Moho surface along profile CC' has been identified by Yan et al. (2001). The Bouguer anomaly is larger oceanwards (Figure 8c). Our Bouguer gravity modeling agrees with the identified Moho surface. The oceanic crust appears after the distance 350 km. The magnetic anomaly generally shows a peak over the oceanic crust (Figure 8c), which corresponds to magnetic anomaly C11 (Figure 1). The TCC

zone is distributed from distance 140 to 350 km. This area is marked by relatively low free-air gravity anomalies.

#### Profile DD' (Figure 8d)

This transect is adopted from the seismic profile of Lüdmann et al. (2001). The interpretation of this seismic profile is controlled by well log data of the Ocean Drilling Program (ODP) sites (Figures 1, 3 and 8d). The basement has been cut by normal faults and the grabens are filled with sediments (Figure 3). No clear intruded or extruded igneous bodies are observed along this transect. Located near the northern end of profile DD', Profile II' shows many normal faults below strata T1 (Figure 6). A clear intruded igneous is found at the distance of about 80 km, which causes topographic upwarping (Figure 6).

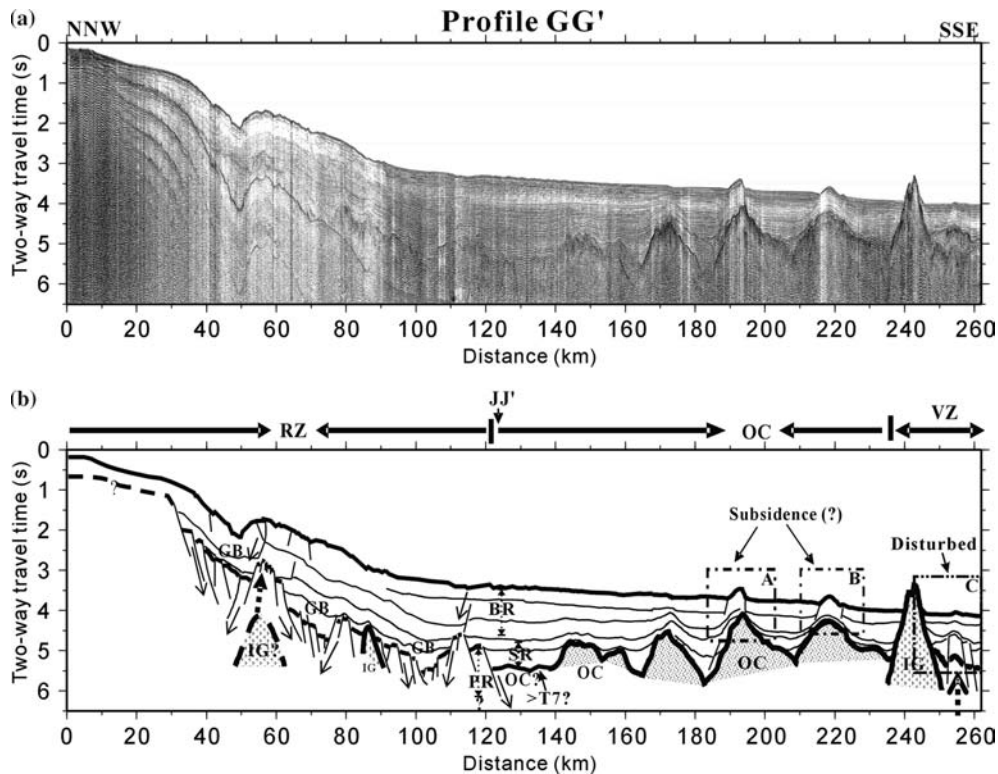


Figure 5. (a) Seismic Profile GG' and (b) the interpretation of profile GG'. There are many normal faults in the continental margin. Oceanic crust is found southward of the distance 130 km. IG: igneous body. OC: oceanic crust. GB: graben. PR: pre-rift. SR: syn-rift. BR: post-rift.

Truncation of sedimentary layers is observed in box T in Figure 6. The uplift around Dongsha Island is possibly due to magmatism.

The Bouguer anomaly along profile DD' increases oceanwards (Figure 8d). Gravity modeling shows that crustal thickness gradually becomes thinner from 0 to 190 km distance (box B in Figure 8d) and is almost constant after 190 km (box A3 in Figure 8d). The magnetic anomaly shows a relatively high anomaly after 190 km distance (box A3 in Figure 8d). We can define the position of COB at the distance of 190 km. Accordingly, the TCC is distributed between the distances from 0 to 190 km.

#### Profile EE' (Figure 8e)

The calculated Bouguer anomaly is also gradually larger oceanwards. We adopt the Moho depth variation defined by Nissen et al. (1995a) to perform the gravity modeling. The result shows a good fitting between the calculated and

synthetic Bouguer anomalies (Figure 8e). Based on the variation of crustal thickness, modelling shows that two significant changes of crustal thickness may be associated with the locations of COB (Figure 8e). The crust after the distance of 380 km is only ca. 6 km thick (box B1 in Figure 8e). The corresponding magnetic anomaly shows high amplitude (box B3 in Figure 8e). We suggest this portion of crust as oceanic. The crust between 250 and 380 km is about 8–12 km thick (box C1 in Figure 8e), somewhat thicker than normal oceanic crust. However, the crustal thickness in this portion is rather constant, without obvious crustal thinning effect. In fact, the profile EE' and the contiguous profile FF' obviously contain intrusive magmatism (Figures 1 and 4). The magmatism may correspond to that near Dongsha Island in middle Miocene (Yao et al., 1994; Ludmann and Wong, 1999). Thus, we agree with the suggestion of Hsu et al. (2005) and move the location of COB to the base of the continental slope (Figure 1).

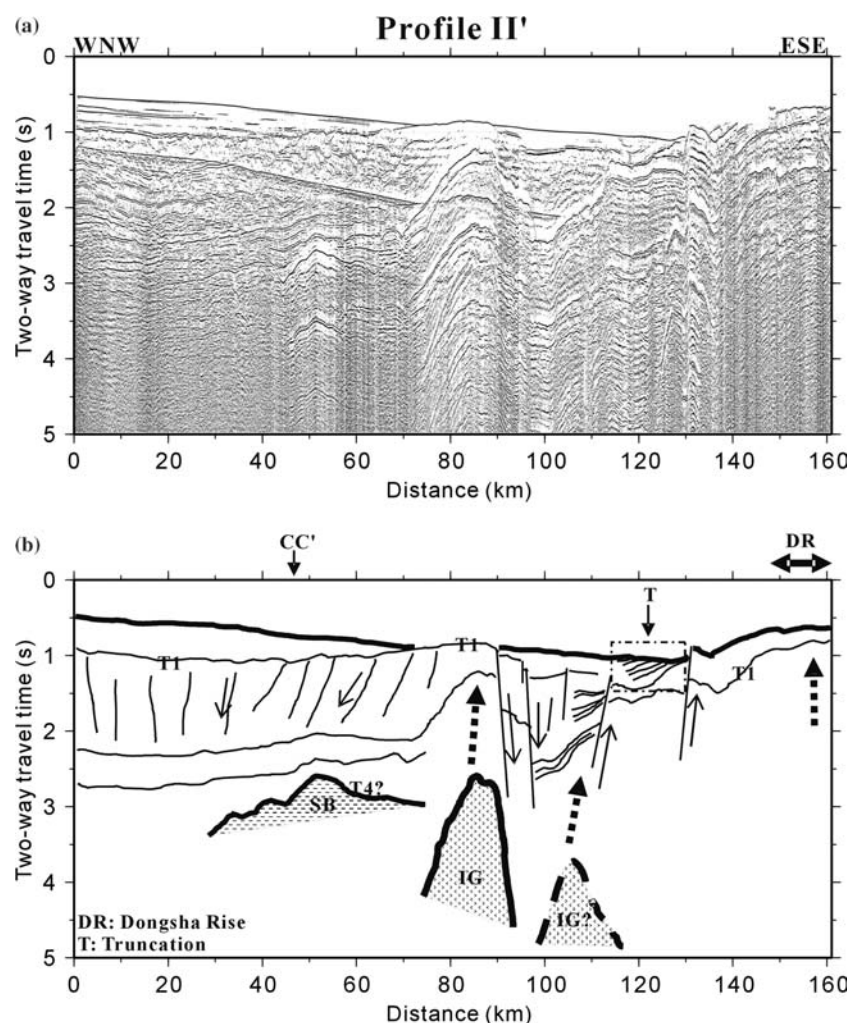


Figure 6. (a) Seismic Profile II' and (b) the interpretation of Profile II'. This profile displays many normal faults below the discontinuity T1. Intruded igneous rock is found at about 80 km distance and has caused topography uplift. Sediment truncation exists close to Dongsha Island (box T). DR: Dongsha Island.

#### Profile FF' (Figure 8f)

The structures along the profile FF' are very similar to those seen in profile EE'. Based on the seismic reflection profile, we can find large scale pre-rift normal faulting in the basement (Figure 4). Surface normal faults can also be observed especially landwards. Gravity modeling shows that the continental crust has been significantly thinned between the distance 0 and 160 km (Figure 8f). However, the magnetic anomaly above the magmatic zone displays some reversal pattern (box C2 in Figure 8f). One magnetic fluctuation corresponds to the magnetic lineations (magnetic anomaly C15) (Figure 1). It implies

that later magmatism did not completely destroy the reversal pattern of the magnetic lineations.

#### Profile GG' (Figure 8g)

The seismic profile of MCS689-5 shows that the oceanic crust is distributed south of distance 120 km (Figure 5). The occurrence of the oceanic crust can also be observed in seismic Profile JJ' which is perpendicular to Profile GG' (Figure 7). Landwards, the basement has been rifted and is associated with tilted, rotated normal faults. Some intrusions also exist beneath the continental slope (Figure 5). Due to subsidence or lateral compression, the seismic sequences in the boxes a

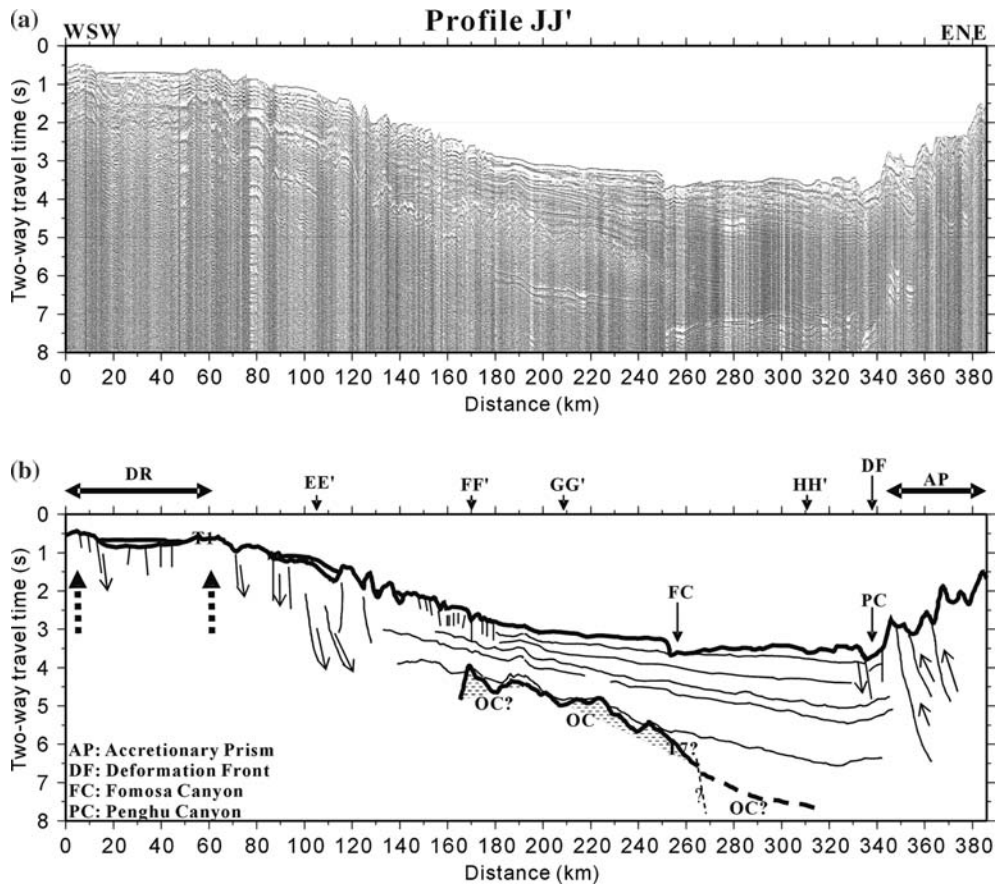


Figure 7. (a) Seismic Profile JJ' and (b) the interpretation of Profile JJ'. Uplift is seen near Dongsha Island. The basement progressively deepens from WSW to ENE. The basement is overlain by thicker sediment in the eastern part of the Formosa Canyon.

and b of Figure 5 display slight warping. Volcano located at ca. 240 km is probably produced in the same way as the 'disturbed zone' in Figure 4. The basement near the volcano is perturbed and a local uplift by thrust faults occurred.

Like the previous sections, the Bouguer anomaly becomes larger oceanwards (Figure 8g). The gravity modeling shows that after distance 90 km crustal thickness is about 8 km and almost remains constant. Based on the analysis of the seismic reflection profile, the COB is located at the distance 120 km; thus, the thin crust between the distance 90 and 120 km is considered as the extension of the thinning crust zone. The magnetic anomaly above the portion of the oceanic crust displays fluctuation pattern corresponding to the reversal pattern of the magnetic anomalies.

#### Profile HH' (Figure 8h)

Profile HH' is the only profile that is located to the east of the LRTPB (Figure 1). Gravity modeling shows that after distance 70 km the modeled crust is extremely thin, only 5–8 km (Figure 8h). The thin crust could be inferred as oceanic crust; however, the magnetic anomaly does not show any signature of magnetic lineation pattern (Hsu et al., 2005). The relatively high magnetic anomaly in box A2 in Figure 8h could be related to local thick crust in that area (box A1 in Figure 8h). The gravity modeling and magnetic signature exhibit contradictory interpretation about the southeast portion of crust. If the thin crust is not oceanic, it implies that there must be anomalous high-density lower crustal material. Alternatively, it is possible that the

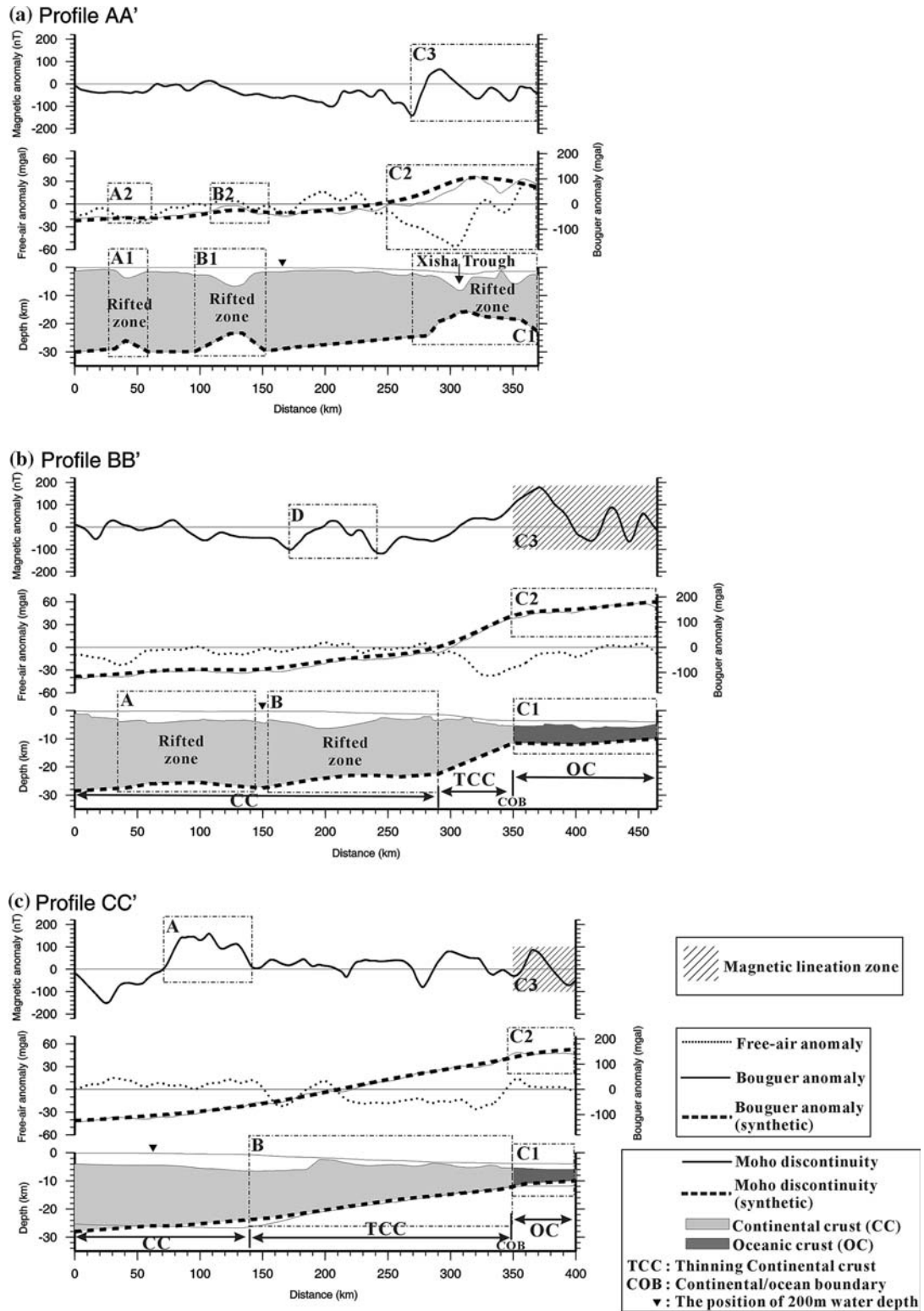
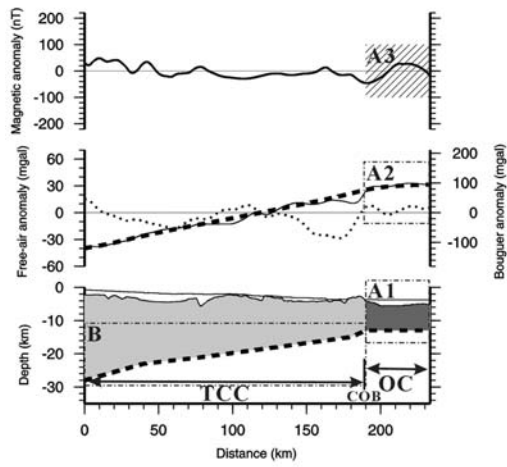
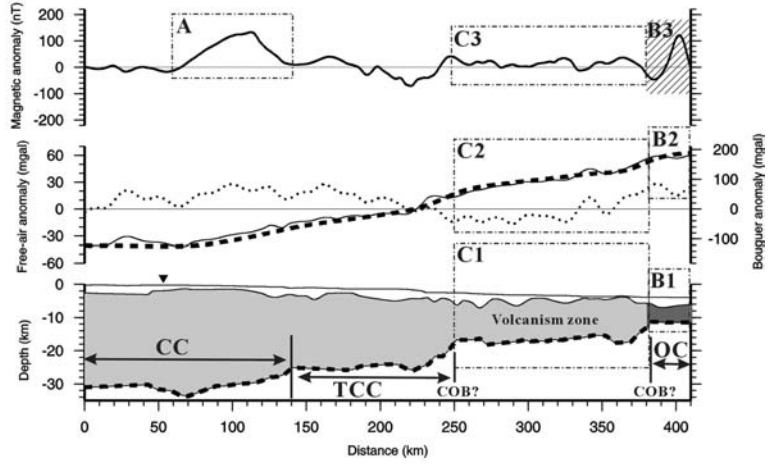


Figure 8. Continued.

(d) Profile DD'



(e) Profile EE'



(f) Profile FF'

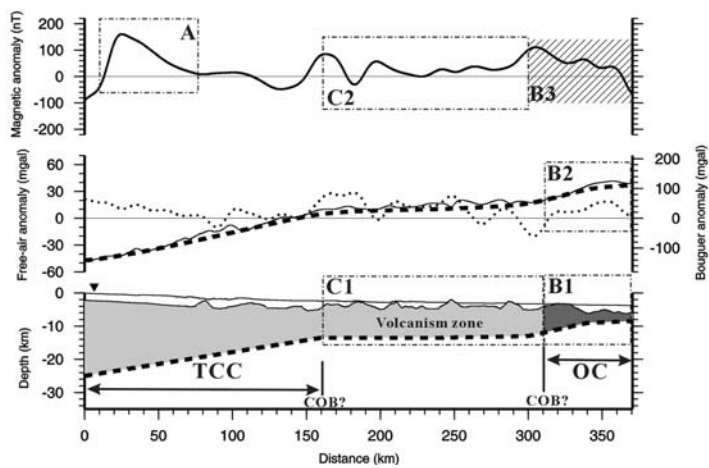


Figure 8. Continued.

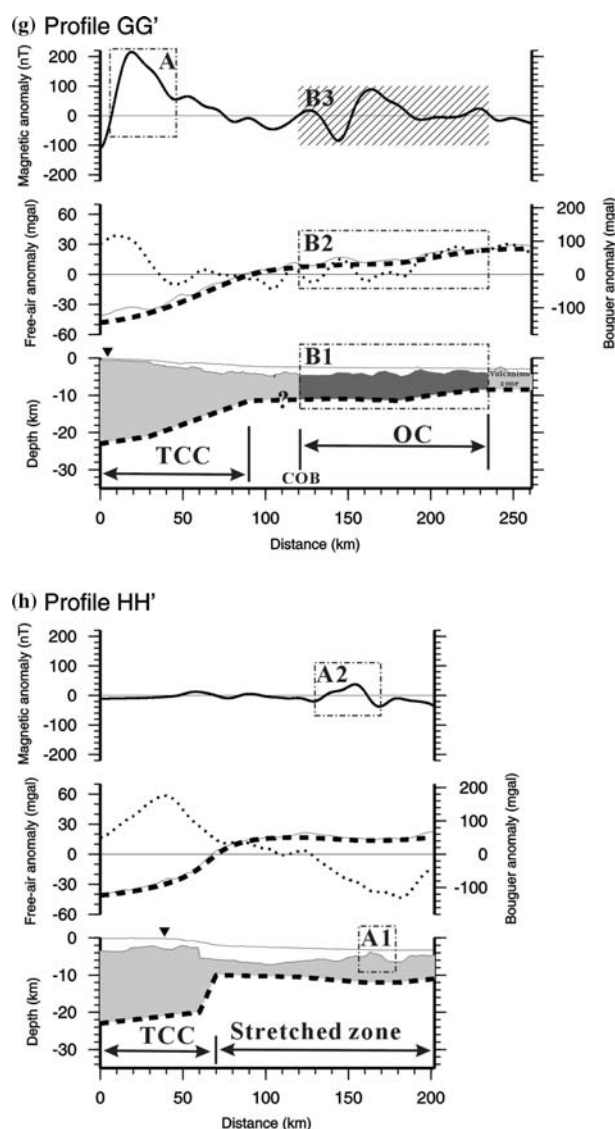


Figure 8. Gravity modeling to find the Moho depth distribution. The location of each profile is shown in Figure 1. The crustal model used for modeling is shown in Figure 2. See text for details.

lineation character of the oceanic crust has been disturbed by post-spreading tectonic events. In that case, the existence of oceanic crust between the LRTPB and Taiwan cannot be excluded.

#### Distribution of Moho depth and crustal thickness

Using the analysis of the above crustal structures, the distribution of continental, thinned continental and oceanic crust in the northern margin of the SCS can be mapped (Figure 9). The unde-

formed or slightly deformed CC zone generally has crustal thickness greater than 20 km. The corresponding Moho depth is greater than 24 km. The TCC zone has a steep slope of the Moho surface that shoals oceanwards. The Moho depth in this zone is from ca. 24 km to 14 km. Probably as a result of tectonic extension, the zone generally reveals relatively low magnetization (Hsu et al., 2005). It explains why relatively high amplitude magnetic anomaly exists near the end of the CC zone (box A in Figures 8c, 8e–8g). The Moho depth of the OC zone is generally from 18 km to

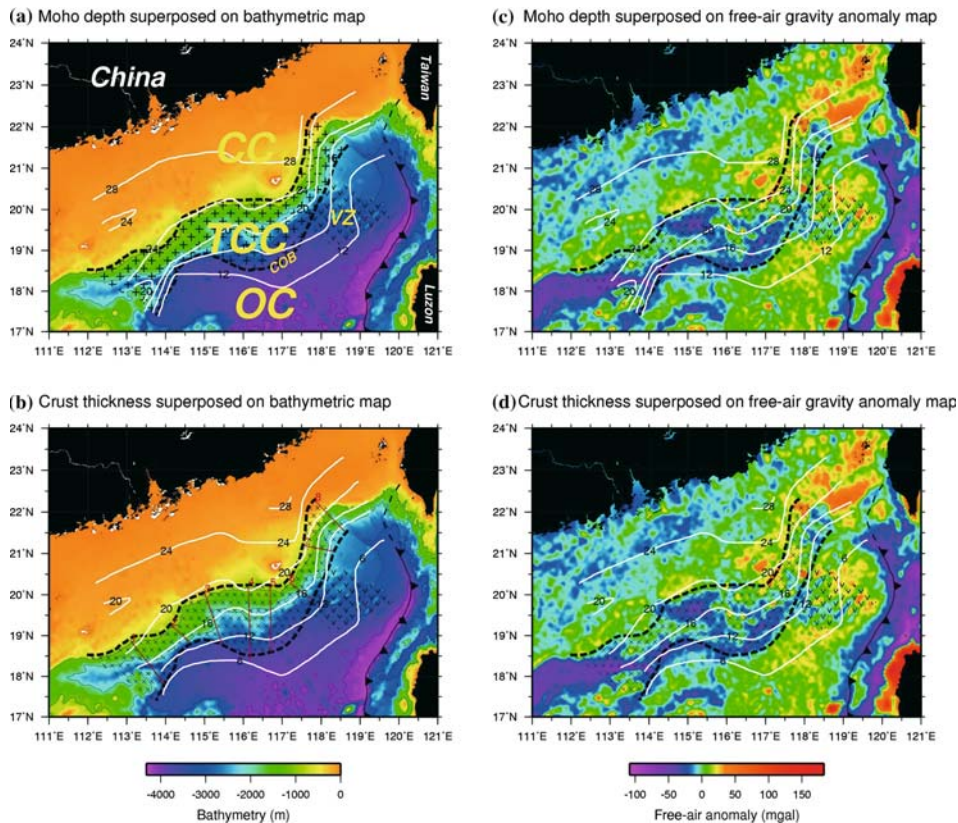


Figure 9. The distribution of Moho depth (km) and crustal thickness (km) of the study region superposed on the bathymetric and gravity anomaly maps, respectively. CC: continental crust zone. TCC: thinned continental crust zone. OC: oceanic crust zone. VZ: volcanic intrusion zone.

8 km and the corresponding thickness of the crust is about 6–9 km. Within the OC domain, some post-spreading volcanism has occurred (e.g. Figures 8e and 8f). The crustal thickness in such volcanic zones is 10–12 km thick. Considering the NE–SW trend of the continental margin, the area around Dongsha Island displays a regional maximum crustal thickness, generally 2 km thicker than the surroundings (Figure 9). Is the reason for the abnormal crustal thickness in this region only due to post-spreading volcanism or due to other mechanisms such as the underplating (Kido et al., 2001) or hotspot volcanism? It needs further investigation.

If we superpose the Moho depth and crustal thickness distributions on the bathymetric map, we can discern that the continental crust starts to thin near the continental shelf break and stops near the base of the continental slope (Figures 9a and 9b). In other words, the COB in the northern SCS generally follows the base of the NE trending

continental slope, rather than the one goes into the Manila Trench as suggested by Briais et al. (1993) (Figure 1). If we superpose the Moho depth and crustal thickness distributions on the gravity anomaly map, we can find that the TCC zone corresponds to a relatively low gravity anomaly zone (Figures 9c and 9d). The low gravity anomaly probably reflects crustal thinning, fracturing, or subsidence.

Based on Figure 9 and the bathymetry, we can deduce the sediment thickness over the region. The map of the average sediment thickness of the region is shown in Figure 10. It indicates that the thickest sediment is deposited in the Pearl River Mouth Basin (cf. Figures 1 and 10). Sediment thicken towards Taiwan (Figure 10), due to flexure of the continental margin and the loading of the Taiwan mountain belt (Yu and Chou, 2001; Lin and Watts, 2002).

To estimate the thinning effect of the continental crust in the northern SCS, we adopt a

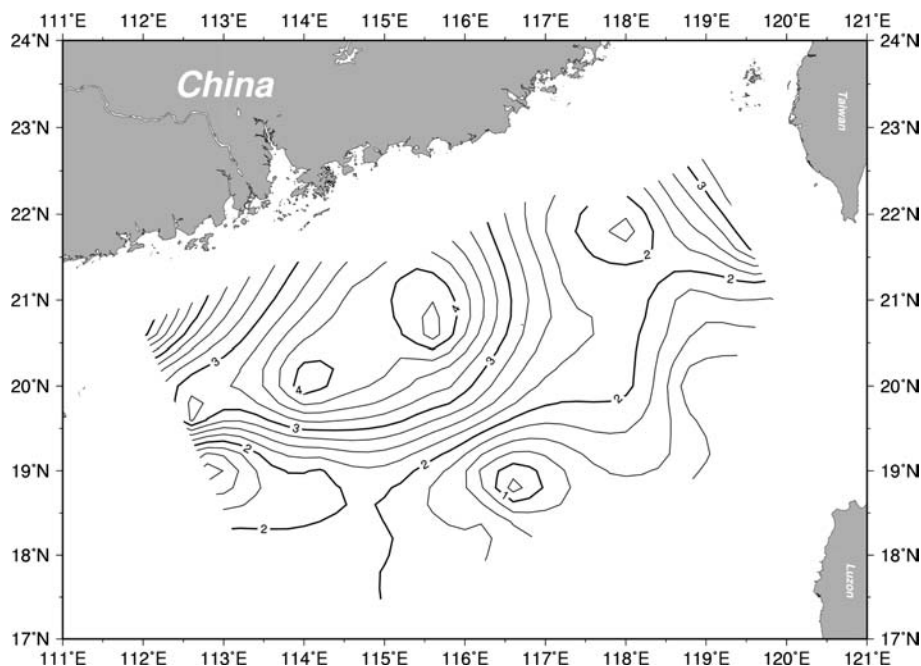


Figure 10. The distribution of the average sediment thickness (km) in the northern continental margin of the SCS.

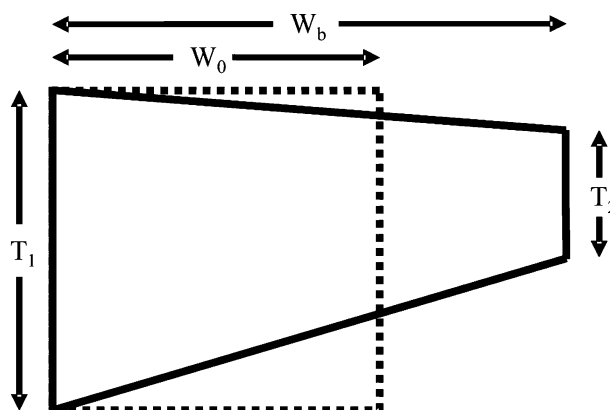


Figure 11. Diagram showing the original crustal block of length  $W_0$  and the stretched block of length  $W_b$ .  $T_1$ : the original continental crust thickness.  $T_2$ : the thickness of the thinned continental crust at the COB.

simple model to compute the continental thinning effect. According to our analyzed crustal sections, the TCC zone usually has a fixed thickness of crust at the end of the CC zone and becomes thinner oceanwards. Considering a trapezoid form of the TCC zone, we can estimate the average thinning effect by defining a thinning factors  $\alpha$ , equal to  $W_b/W_0$ , and  $T_1$  represents the crustal thickness of the CC zone and  $T_2$  is the crustal thickness near the beginning of

the OC zone (Figure 11). In other words, we consider that the thinned area  $(T_1 + T_2) \times W_b/2$  is equal to the original undeformed area  $T_1 \times W_0$ . We have estimated the  $\alpha$  at the locations parallel to the true crustal slope (indicated by red lines in Figure 9b). The results show that the values of thinning factors  $\alpha$  in the northern continental margin of the SCS are between 1.14 and 1.50 (Table 2). It indicates that the rifting rates in northern continental margin of the SCS

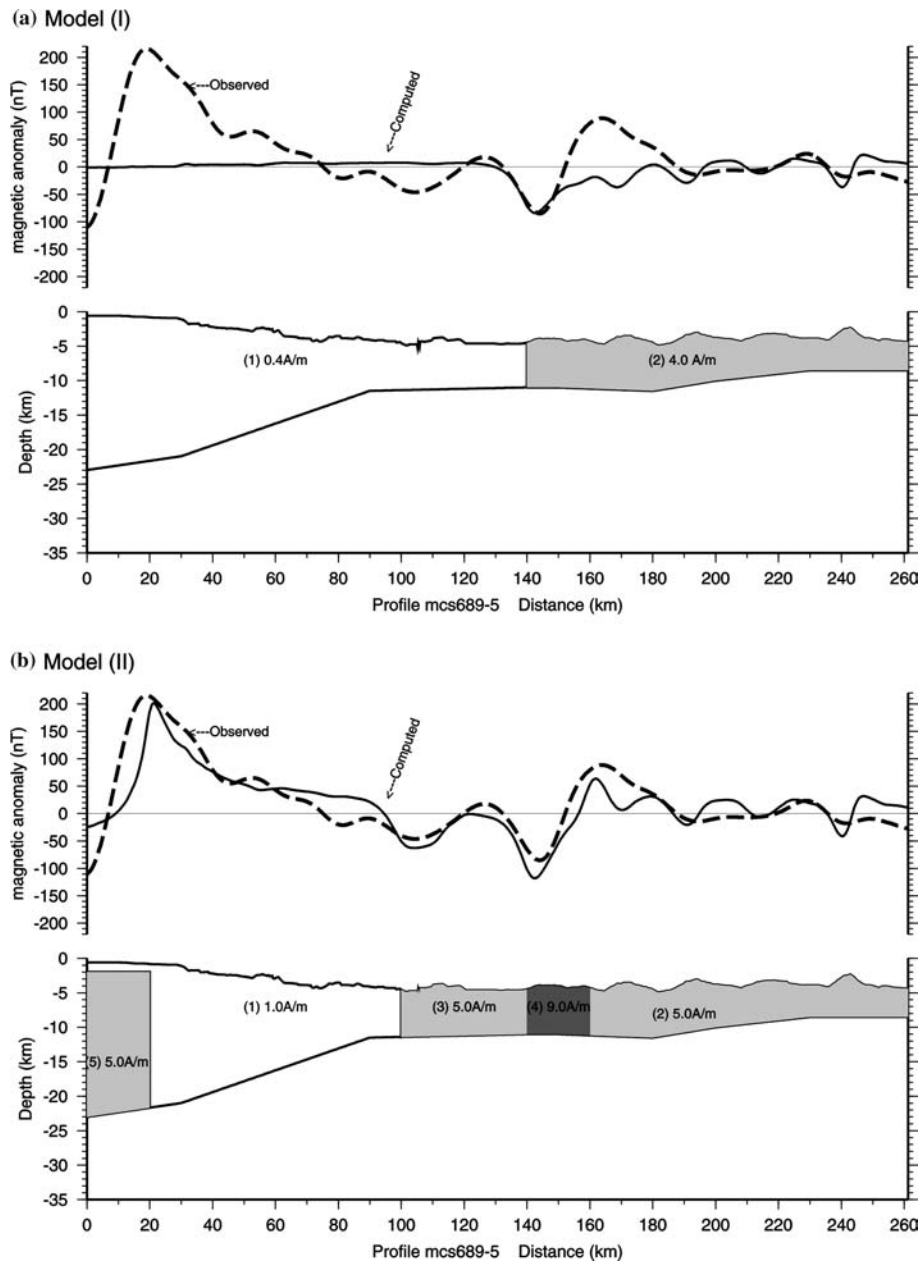


Figure 12. The magnetic model of profile GG'. Model (I) is a simple model containing two parts: oceanic (box (2)) and continental crust (box (1)). Model (II) is a more complex model and suggests a high magnetization at distance 10 km and at 150 km. See text for discussion.

are not regular. The large thinning factors in the south of the Dongsha Island and in the Xisha Trough not only indicate large extension but also imply the exhumation of the upper mantle.

#### Characteristics of the continent–ocean transition

The transition zone in Lofoten volcanic margin of the north Atlantic shows that the seismic velocities of crust gradually decrease from oce-

Table 2. The continental thinning of the northern margin of the SCS. The profile locations used for estimation are marked by red lines in Figure 9b.

Line number	T <sub>1</sub> (km)	T <sub>2</sub> (km)	W <sub>b</sub> (km)	W <sub>0</sub> (km)	Thinning factor ( $\alpha = W_b/W_0$ )
1	24	8	146.66	97.77	1.50
2	19	14	73.33	63.68	1.15
3	19	12	119.16	97.21	1.23
4	20	8	192.50	134.75	1.43
5	20	10	183.33	137.50	1.33
6	20	15	73.33	64.16	1.14
7	24	12	77.00	57.75	1.33
8	24	12	110.00	82.50	1.33

anic crust above the SDRs (seaward dipping reflectors) into continental crust (Mjelde et al., 1996). In contrast a serpentinized ridge corresponding to serpentinized peridotite was found in the west Iberia non-volcanic margin (e.g. Sibuet et al., 1995; Pinheiro et al., 1996). However, those characters are not identified in northern margin of the SCS. To better understand the transition character in the northern SCS, we further perform a magnetic modeling along the profile GG' (Figure 8g). Benes et al. (1997) has indicated a large variation of the oceanic magnetization from 4 to 22 A/m and suggested inhomogeneous oceanic crust. Considering the present-day magnetization direction, we assume that the magnetization magnitude for the oceanic crust is 4 and 0.4 A/m for the continental crust (Figure 12a). In that case, we find that the magnetic anomalies in the continental or oceanic parts are not fitted well. Using forward modeling, we find that the CC zone must be a relatively high magnetization material (area 5 in Figure 12b) and near the COB there must be a high magnetization material in the oceanic crust (area 4 in Figure 12b). Alternatively, we can interpret that the TCC zone as being a relatively low magnetization (area 1 in Figure 12b). As mentioned previously, the TCC zone could suffer from thinning or fracturing of the crust and cause the diminution of magnetization. In that case, the high magnetic anomaly along the northern continental margin of the SCS is a consequence of strong magnetization contrast. The reason for the high magnetization in area 4 in Figure 12b is still questionable. Since no peridotite ridge is found in this region, it could not be serpentinized peridotite. Otherwise,

it could be interpreted as the result of magnetic polarity reversals in the oceanic crust.

### Conclusion

The crustal structure in the northern continental margin of the SCS generally displays a NE–SW trend. We distinguish three zones in: the less deformed CC zone, the TCC zone, and the OC zone. The TCC zone has the steep slope of the Moho surface that becomes shallow oceanwards from about 24 km deep to about 14 km deep. The corresponding crustal thickness is from about 20 km thick to about 10 km thick. The distribution of the TCC zone also displays relatively low free-air gravity anomalies. The existence of oceanic crust in the northernmost SCS is evidenced by seismic reflection data. Accordingly, the COB in the northern SCS is suggested to be along the base of the continental slope. Some area exhibits thicker oceanic crust probably because of post-spreading igneous intrusions. The area around Dongsha Island displays a regional maximum of the crustal thickness and the Moho depth. The crustal nature of the northernmost portion of the continental margin, close to the Taiwan orogen, is still ambiguous.

### Acknowledgements

We thank the crew of the R/V Ocean-Research I for helping collect MCS data during ORI-620 and MCS689 cruises. The authors thank Peter

Clift and Tan K. Wang for their thoughtful reviews which significantly improved the original paper. Discussions with J.-C. Sibuet and A.T. Lin are helpful. This study is under the Grant of National Science Council, Taiwan, R.O.C. The GMT software package was used to display some of the figures (Wessel and Smith, 1995).

## References

- Benes, V., Bocharova, N., Popov, E., Scott, S. D. and Zonenshain, L., 1997, Geophysical and morpho-tectonic study of the transition between seafloor spreading and continental rifting, western Woodlark Basin, Papua New Guinea, *Marine Geol.* **142**, 85–98.
- Briais, A., Patriat, P. and Tapponnier, P., 1993, Updated interpretation of magnetic anomalies and seafloor spreading stages in the South China Sea: Implications for the tertiary tectonics of Southeast Asia, *J. Geophys. Res.* **98**, 6299–6328.
- Clift, P. D., Lin, J. and ODP Leg 184 Scientific Party, 2001, Patterns of extension and magmatism along the continent-ocean boundary, South China margin, in: Wilson, et al. R. C. (ed.) *Non-Volcanic Rifting of Continental Margins: a Comparison of Evidence from Land and Sea*, Geological Society, London, Special Publication **187**, 489–510.
- Henkart, P., 1992, *SIOSEIS – a Computer System for Enhancing and Manipulating Marine Seismic Reflection and Refraction Data*, Scripps Institute of Oceanography.
- Hsu, S.-K., Liu, C.-S., Shyu, C.-T., Liu, S.-Y., Sibuet, J.-C., Lallemand, S., Wang, C., and Reed, D., 1998, New gravity and magnetic anomaly maps in the Taiwan-Luzon region and their preliminary interpretation, *TAO* **9**, 509–532.
- Hsu, S.-K., Yeh, Y.-C., Doo, W.-B. and Tsai, C.-H., 2005, New identification of magnetic lineations and bathymetry in the Northernmost South China Sea and their tectonic insights, *Marine Geophys. Res.* (this issue).
- Kido, Y., Suyehiro, K. and Kinoshita, H., 2001, Rifting to spreading process along the Northern continental margin of the South China Sea, *Marine Geophys. Res.* **22**, 1–15.
- Lin, A. T. and Watts, A. B., 2002, Origin of the west Taiwan basin by orogenic loading and flexure of a rifted continental margin, *J. Geophys. Res.* **107**, doi:10.1029/2001JB000669.
- Ludmann, T. and Wong, H. K., 1999, Neotectonic regime on the passive continental margin of the northern South China Sea, *Tectonophysics* **311**, 113–138.
- Ludmann, T., Wang, H. K. and Wang, P., 2001, Plio-Quaternary sedimentation processes and neotectonics of the northern continental margin of South China Sea, *Marine Geol.* **172**, 331–358.
- Ludwig, W. J., Kumar, N. and Houtz, R. E., 1979, Profiler-sonobuoy measurements in the South China Sea Basin, *J. Geophys. Res.* **84**, 3505–3518.
- Mjelde, R., Kodaira, S., Hassan, R. K., Goldschmidtrokita, A., Tomita, N., Sellevoll, M. A., Hirschleber, H. B., Shimamura, H., Iwasaki, T. and Kanazawa, T., 1996, The continent/ocean transition of the Lofoten volcanic margin, N. Norway, *J. Geodyn.* **22**, 189–206.
- Nissen, S. S., Hayes, D. E., Buhl, P., Diebold, J., Yao, B., Zeng, W. and Chen, Y., 1995a, Deep penetration seismic soundings across the northern margin of the south China Sea, *J. Geophys. Res.* **100**, 22407–22433.
- Nissen, S. S., Hayes, D. E., Yao, B., Zeng, W., Chen, Y. and Nu, X., 1995b, Gravity, heat flow, and seismic constraints on the processes of crustal extension: Northern margin of the South China Sea, *J. Geophys. Res.* **100**, 22447–22483.
- Pinheiro, L. M., Wilson, R. C. L., Pena dos Reis, R., Whitmarsh, R. B. and Ribeiro, A., 1996, The western Iberia margin: a geophysical and geological overview, *Proceedings of the Ocean Drilling Program: Scientific Results* **149**, 3–23.
- Sandwell, D. T. and Smith, W. H. F., 1997, Marine gravity anomaly from Geosat and ERS-1 satellite altimetry, *J. Geophys. Res.* **102**, 10039–10050.
- Sibuet, J.-C. and Hsu, S.-K., 1997, Geodynamics of the Taiwan arc-arc collision, *Tectonophysics* **274**, 221–251.
- Sibuet, J.-C., Hsu, S.-K., Pichon, X. L., Formal, J. P. L., Reed, D., Moore, G. and Liu, C.-S., 2002, East Asia plate tectonics since 15 Ma: Constraints from the Taiwan region, *Tectonophysics* **344**, 103–134.
- Sibuet, J.-C., Louvel, V., Whitmarsh, R. B., White, R. S., Horsefield, S. J., Sichler, B., Leon, P. and Recq, M., 1995, *Constraints on Rifting Processes from Refraction and Deep-Tow Magnetic Data: The Example of the Galicia Continental Margin (West Iberia). Rifted Ocean-Continent Boundaries*. Netherlands: Kluwer Academic Publishers, pp. 197–218.
- Taylor, B. and Hayes, D. E., 1983, Origin and history the South China Sea, in Hayes, D. E. (ed.), *The Tectonic and Geologic Evolution of Southeast Asia Seas and islands*, 2, Geophysical Monographic Series, 27, Washington, DC: AGU.
- Wessel, P. and Smith, W. H. F., 1995, New version of the Generic Mapping Tools released. *Eos Trans., AGU (Suppl.)* **76**, 329.
- Yan, P., Zhou, D. and Liu, Z., 2001, A crustal structure profile across the northern continental margin of the South China Sea, *Tectonophysics*, **338**, 1–21.
- Yao, B., Zeng, W., Hayes, D. E. and Spangler, S., 1994, *The Geological Memoir of South China Sea Surveyed Jointly by China and the U.S.A.*, Wuhan: The Press of Chinese Geological University.
- Yu, H.-S., and Chou, Y.-W., 2001, Characteristics and development of the flexural forebulge and basal unconformity of western Taiwan foreland basin, *Tectonophysics* **333**, 277–291.